THE PLASMA BEAT WAVE ACCELERATOR - EXPERIMENTS

C. Joshi

University of California, Los Angeles, CA 90024, U.S.A.

ABSTRACT

In the Plasma Beat Wave Accelerator, acceleration is achieved by a longitudinal electrostatic field produced as a result of charge separation generated by a plasma wave traveling close to the speed of light. The plasma wave in turn is produced by two colinear laser pulses whose frequency difference is such that the beat frequency matches the plasma frequency. Optical mixing and Raman forward scattering instability play a crucial role in the growth and nonlinear saturation of such high phase velocity plasma waves. In this paper we describe experiments that show, i) that long wavelength high phase velocity electron plasma waves can be generated in a quasi-homogeneous plasma by optical mixing, ii) relativistic particles are indeed generated by the Raman forward instability, and iii) with short wavelength lasers, potential exists for obtaining ultra-high electric fields.

INTRODUCTION

Collective particle accelerators making use of the high fields associated with focused laser beams have received considerable attention in recent years. Although the transverse electric fields at the focus can be as high as 10^9-10^{10} volts per meter, a charged particle oscillating in such a field achieves no net acceleration at all since there is no component of the electric field in the direction of propagation. To circumvent this problem it has been suggested that the electrostatic field of a longitudinal plasma oscillation set up by the electromagnetic wave can be used to accelerate particles.

In a laboratory plasma with no external magnetic field there are basically three processes which give rise to high frequency plasma oscillations. The first is a linear mode conversion process, also known as resonant absorption because it occurs when the frequency of the laser light matches the local plasma frequency in an inhomogeneous plasma. The energy in the plasma wave is then coupled to plasma electrons by collisional damping, Landau damping, electron trapping and wavebreaking. Since the phase velocity of the resonant field propagates towards the lower density region, the wave particle interaction preferentially accelerates electrons down the density gradient. Although this process can produce very large electric fields (10^{10}-10^{11} volts/cm), the region of resonance is very narrow and consequently particles are not accelerated to ultra-relativistic energies.

The second mechanism is known as high frequency parametric instabilities in which an electromagnetic wave propagating in an underdense plasma undergoes a decay into an electron plasma wave and another electromagnetic wave(Stimulated Raman Scattering), or an ion acoustic wave (Parametric Decay Instability) or another electron plasma wave (Two-Plasmon Decay). Whenever one of the decay products is an electron plasma wave, very large electric fields in the direction of propagation can be produced. Poisson's equation gives $\nabla \cdot E_p = -4\pi e n_1$ and the maximum amplitude of the electron plasma wave is obtained when the level of density fluctuation $n_1/n_o = 1$. Thus $k_p E_p = -4\pi e n_o$ and using $\omega_p = 4\pi n_o e/m$ we obtain the electric field

$E_p = m\omega_p v_p/e$ and the wave potential $e\phi$ as mv_p^2 where v_p is the phase velocity of the wave. For $v_p = c$, $e\phi = \gamma mc^2$. In the nonrelativistic case, a particle whose velocity v_e in the direction of propagation of the wave is near the phase velocity can be trapped and gain up to $4mv_p^2(v_e/v_p)^{\frac{1}{2}}$. In the relativistic case $v_p \simeq c$ and the maximum energy gained is theoretically up to $(\omega^2/\omega_p^2)mc^2$.

The third mechanism is known as optical mixing in which two electromagnetic waves beat in a plasma to resonantly drive density fluctuations. The electrostatic field of such a resonantly driven plasma wave can be very large and be used to accelerate the plasma electrons or an injected group of particles. One can think of the optical mixing process as Raman scattering instability below threshold but with finite noise source, or alternatively, nonlinear saturated limit of Raman forward scattering.

In this paper we shall discuss the optical mixing process and the stimulated Raman forward scattering instability. In particular, we shall examine the role of these in the Plasma Beat Wave Accelerator. In the Plasma Beat Wave Accelerator, acceleration is achieved by an electrostatic field produced as a result of charge separation generated by a plasma wave traveling close to the speed of light. The plasma wave in turn is produced by colinear two laser pulses whose amplitude is modulated so that the beat frequency matches the plasma frequency. Experiments that show that long wavelength and high phase velocity electron plasma waves can be generated by the optical mixing process in a homogeneous plasma as well as generation of ultra-relativistic particles by the Raman instability are described.

OPTICAL MIXING

The nonlinear excitation of electron plasma waves (EPW) by beating two electromagnetic (EM) waves has been under considerable investigation lately because of its potential role in the laser-electron accelerator,[1] cascade plasma heating,[2] laser-fusion pellet preheat,[3] and as a plasma density diagnostic.[4] Basically, when two coherent EM waves, (ω_o, k_o) and (ω_1, k_1), occupy the same volume the total intensity is modulated in space at $\Delta k = k_o \pm k_1$, and in time at $\Delta\omega = \omega_o \pm \omega_1$. The ponderomotive force (F_{NL}) in a plasma associated with this beat wave can resonantly drive longitudinal electron density fluctuations of wavenumber $k_p = \Delta k$, if $\omega_{EPW} = \Delta\omega$. ω_{EPW} is the frequency of the electron plasma wave and is related to the plasma frequency via the dispersion relation $\omega_{EPW}^2 = \omega_p^2 + 3k_p^2v_e^2$. This is the usual optical mixing process. If the two EM waves are colinear as shown in Fig. 1, then the phase velocity $v_p = \omega_{EPW}/k_p$ at which the density fluctuations propagate is nearly equal to the group velocity of the EM waves, $v_g = c(1 - \omega_p^2/\omega_o^2)^{\frac{1}{2}}$, and the three waves are locked into synchronism over thousands of wavelengths if $\omega_p >> \omega_o$. Also, since $v_p \simeq c$ there is little Landau damping and the EPW can grow to a very large amplitude.

The behavior of such large amplitude plasma waves driven by beating of two laser beams has been studied by Rosenbluth and Liu.[5] They found that for $v_o/c << 1$, $\tilde{n}/n_o << 1$, the density fluctuations grow linearly with time when $\omega_p = \Delta\omega$.

$$\frac{\tilde{n}}{n_o}(t) = \frac{\tilde{n}}{n_o}(t=0) + \frac{1}{4}\,\frac{v_{o(0)}}{c}\,\frac{v_{o(1)}}{c}\,\omega_p t \qquad (1)$$

Where $\tilde{n}/n_o$ is the EPW amplitude and $v_{o(0,1)} = eE_{(0,1)}/m\omega_{(0,1)}$ is the electron quiver velocity in the laser fields. Wavebreaking is approached when $\tilde{n}/n_o \to 1$; however, to reach this limit the EPW must be exactly in

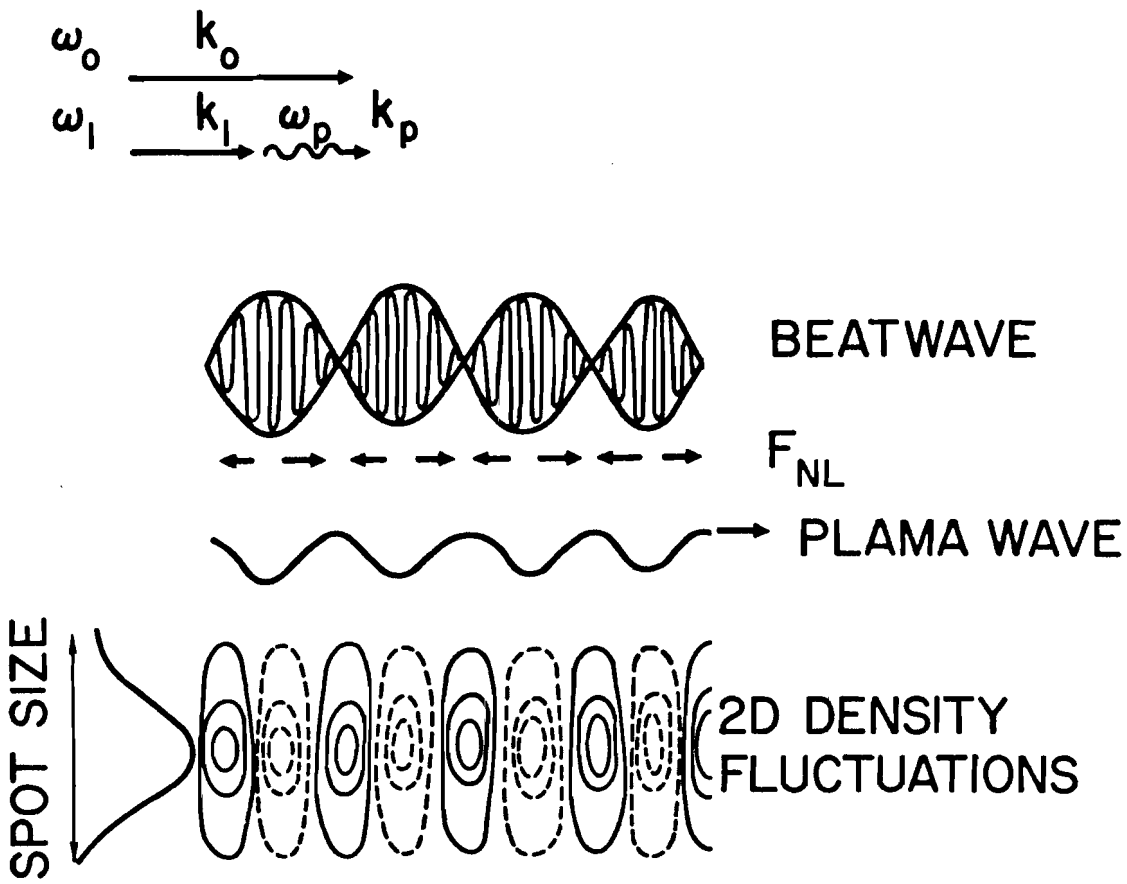

Fig. 1. Resonant excitation of an EPW (ω_{EPW}, k_p) by beating two EM waves (ω_o,k_o) and (ω_1, k_1). Because of the finite spot size, the density fluctuations are 2D with solid lines (dotted lines) representing contours of increasing (decreasing) density.

phase with the beat wave. As $\tilde{n}/n_o \to 1$, relativistic effect on the frequency mismatch becomes important and the EPW saturates at a lower amplitude given by

$$(\tilde{n}/n_o)_{max} \simeq \frac{1}{16}\left(\frac{v_{o(0)}}{c}\ \frac{v_{o(1)}}{c}\right)^{1/3}. \qquad (2)$$

If v_o/c is O(1) for one or both the beams, then the threshold for the stimulated Raman forward scattering (RFS) instability may be exceeded in which case relativistic effects do not provide the saturation mechanism for the EPW.

RAMAN FORWARD SCATTERING INSTABILITY

RFS instability is basically the decay of an incident EM wave into a forward propagating EM wave and an EPW with the usual energy and momen-

tum conservation condition:

$$\omega_o = \omega_1 + \omega_{EPW}$$
$$k_o = k_1 + k_p \cdot \qquad (3)$$

The threshold for the RFS instability is rather high in an inhomogeneous plasma[6]

$$I\lambda_\mu^2 \gtrsim 5\times10^{17}(n_c/n)^2\ (\Delta n/n_c)\ (\lambda/\Delta x)\ Wcm^{-2}\mu^2 \qquad (4)$$

where the density changes by Δn in a length Δx at an average density n. However, once this threshold is exceeded, the long wavelength high phase velocity EPW can grow rapidly. Relativistic effects do not provide a saturation mechanism because the change in ω_p can be adjusted out by a change in the frequency of the forwards scattered light ω_s. Thus in the two beam case, the density fluctuations driven by optical mixing will act as an enhanced noise source to vigouously drive RFS provided that the threshold intensity is exceeded. The other one-dimensional instability competing with RFS is the Raman backscatter (RBS). By solving the dispersion relation[7]

$$1 - Z'/(2k^2\lambda_D^2) = Z'v_o^2/[8\lambda_D^2(c^2k^2 \pm 2kk_oc^2 \pm 2\omega\omega_o - \omega^2)], \qquad (5)$$

where Z' is the Fried-Conte function and λ_D is the electron Debye length, the growth rate for the two instabilities can be found.[8] This is shown in Fig. 2. In a cold plasma, RBS dominates; however, in a hot underdense plasma, the growth rates for the two instabilities become comparable. The longitudinal E field associated with the high phase velocity EPW characteristic of RFS can be very high and is responsible for accelerating either the plasma electrons or externally injected particles to ultra-relativistic energies. This mechanism, known as "trapping", can be more severe

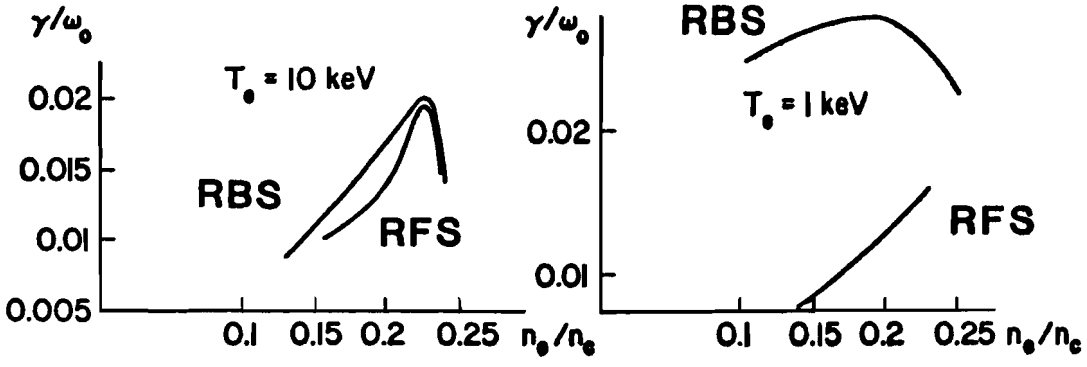

Fig. 2. The normalized growth rates for the RFS and RBS at different densities in a homogeneous plasma. $v_o/c \sim 0.1$ (Ref.8)

than Landau damping. (Fig. 3) Landau damping is strong when v_p is $0(v_e)$ because the slope of the electron distribution function $(\partial f/\partial v)_{v_e}$ has a maximum near the thermal velocity. Landau damping results in the local flattening of the distribution function in the vicinity of v_p thereby producing a heated tail of (nonrelativistic) electrons. However, when $v_p >> v_e$ Landau damping is small. Furthermore, when the amplitude of such a high phase velocity EPW is small, there are very few electrons in the background thermal distribution which are near enough to the phase velocity to be trapped. However, as pointed out by Dawson and Shanny,[9] electron trapping is a nonlinear damping mechanism not local in velocity space. As the wave amplitude increases, the number of particles that can interact with the wave increases rapidly. Consequently, the damping can be much larger than that predicted by the linear theory. The trapping width[10] is given by $v_t = (2eE_p v_p/m\omega_p)^{\frac{1}{2}}$. Electrons or externally injected particles with velocity close to the phase velocity will be accelerated to $\simeq c$. Since v cannot exceed c, a small change in v/c greatly increases the relativistic $\gamma = (1 - v^2/c^2)^{-\frac{1}{2}}$ so that particles with very large energies can be produced.

The saturation mechanism for the EPW driven by RFS instability is thus particle trapping. Pump depletion should not be a problem since the energy given to the forward scattered EM wave is much greater than that to the EPW. This is dictated by the Manley-Rowe relation or the law of conservation of wave action. Viz:

$$\frac{w_o}{\omega_o} = \frac{w_1}{\omega_1} = \frac{w_{EPW}}{\omega_{EPW}} \tag{6}$$

where $w_j = N_j \hbar\omega$ and N_j is the change in number of quanta of the jth wave.

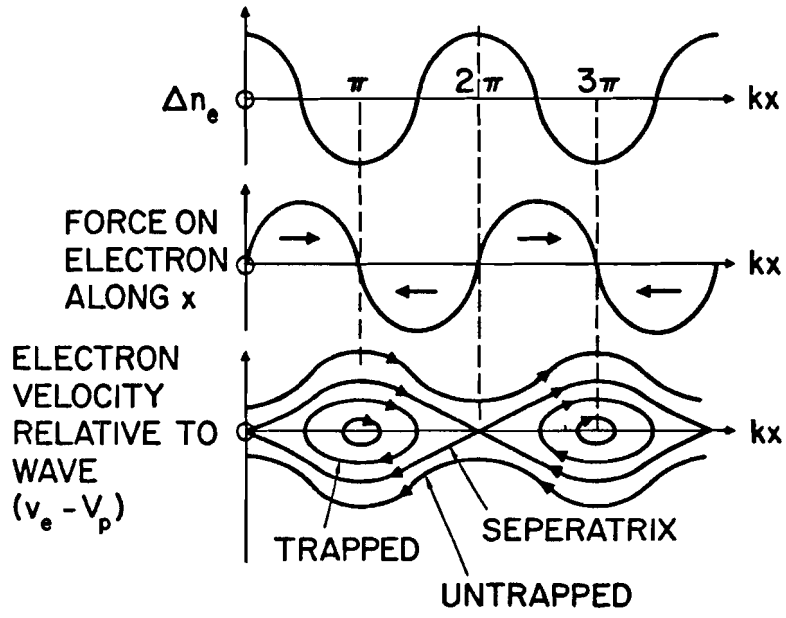

Fig. 3. Trapped particle orbits in an electron plasma wave. The frame of reference is moving at v_p along x.

Since repeated k matching is possible for the RFS instability it can be argued that pump depletion is only important when the original EM wave has cascaded down by multiple RFS to waves near ω_p. The other saturation mechanism such as harmonic generation, wave-wave coupling, ion dynamics and mainbody heating followed by increased Landau damping may also be significant. In realistic experimental situations Raman sidescattering, filamentation, self-generated B fields due to the electron beam and density inhomogeneities may also influence the RFS instability. Computer simulations using relativistic electromagnetic particle codes [11,12] is the only readily available tool to investigate these competing phenomena.

EXAMPLE

The 10.6 μ and 10.27 μ lines of the CO_2 laser can beat in a plasma to resonantly couple with a plasma density of $\sim 10^{16}$ cm^{-3} which is 0.1% of the critical density ($n/n_c \sim 10^{-3}$). The laser light group velocity is $\sim(1 - \frac{1}{2}\omega_p^2/\omega_o^2)c$. This equals the phase velocity of the plasma wave. In the wave frame a trapped electron travelling with v_p thus has a relativistic $\beta = 1 - \omega_p^2/2\omega_o^2$. Its relativistic γ is equal to $(1 - \beta^2)^{-\frac{1}{2}} = \omega_o/\omega_p$. However, transforming the energy of the trapped electron from the wave to the laboratory frame we find that the maximum energy gained is $2\gamma^2 mc^2 = (2\omega^2/\omega_p^2)mc^2$ which is about one GeV. The length to reach this energy is approximately $(2\omega^2/\omega_p^2)(c/\omega_p)$ which is about 10 cm. This places a rather severe requirement on the density homogeneity of the plasma source and the focusing of the two laser beams, but both can be achieved using present day technology. The level of density fluctuations required to obtain an accelerating electric field of 10 GeV per meter can be estimated using the Poissons equation and the optical mixing formula in the relativistic limit given by equation (2) is then used to roughly calculate the laser intensity required. This leads to $I_o = I_1 = 1.4 \times 10^{16}$ Wcm^{-2} or $v_o(1)/c = v_o(0)/c \simeq 1$. Incidentally, this intensity will exceed the <u>inhomogeneous</u> RFS instability threshold even if we assume a 10% density ripple per cm.

EXPERIMENTS

Although simple in principle, optical mixing is not straight-forward in practice. In fact, until very recently there had been only one experiment[13] in which resonantly driven density fluctuations using two laser frequencies were diagnosed using a probe beam to Thomson scatter of the density fluctuations. In any case, the signal to noise ratio of the Thomson scattered light was only about 3. Diagnosing the EPW driven by colinear laser beams with the condition $\omega_p << \omega_o$ is a tremendously difficult problem because of the short k_p. Also, one must have either a well controlled multiline laser or a tunable laser and a <u>homogeneous</u>, tunable density plasma source. By inserting a 10 cm long SF_6 cell inside a gain-switched TEA CO_2 laser oscillator and varying the SF_6 pressure it is possible to obtain controlled multiline operation mainly on 10.6 μ lines in the P(20) band, 10.27 μ lines in the R(16) band and the 9.6 μ lines in the P(20) band. Each band contains 3 to 5 lines each ~40 GHz apart of roughly the same intensity (within a factor of 5). This is shown in Fig. 4. The frequency difference between the 9.6 μ and 10.27 μ gives $\omega_p = 1.35 \times 10^{13}$ Hz corresponding to $n_e = 5.7 \times 10^{16}$ cm^{-3}.

For a tunable density source one can either use a θ pinch or a pulsed arc plasma. Density homogeneity required can be obtained in a θ pinch in a fully ionized H_2 or He plasma whereas one has to use a heavy gas such

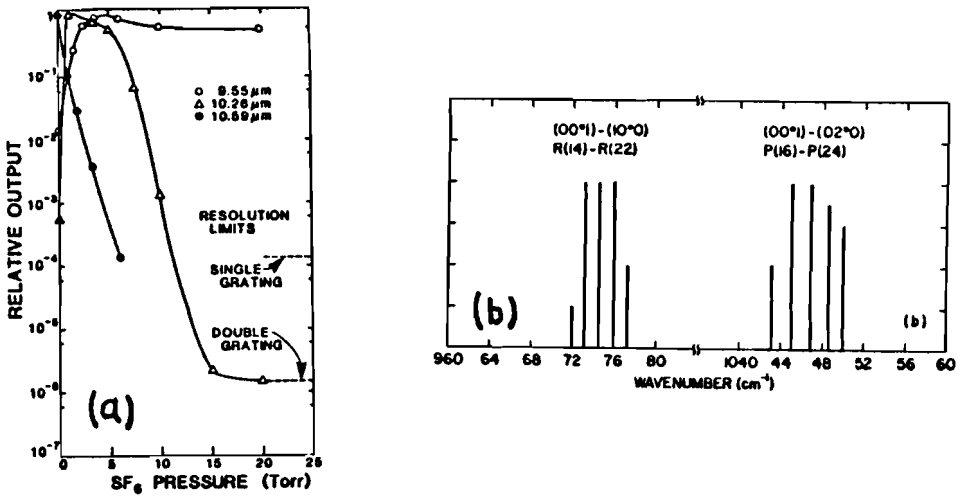

Fig. 4. Multiline operation of a CO_2 oscillator (a) and fine structure of the $R(16)_{10.27\ \mu}$ and $P(20)_{9.6\ \mu}$ bands (b).

as N_2 or Ar in an arc. Fig. 5 shows the density evolution as a function of time of a 4 Torr, 5 eV Ar plasma produced by a pulsed capacitive arc. The axial density profile measured interferometrically showed that, within the limits of measurement accuracy the condition $\Delta\omega = \omega_p$ can be achieved over the depth of focus of the f/7.5 lens.

The laser beam (75 ns FWHM) containing roughly equal powers in the 9.6 μ and 10.27 μ lines was focused to an intensity of 10^{10} Wcm^{-2} by an f/7.5 lens to a 300 μ spot on the plasma axis. The transmitted light plus any forward scattered light was collected by an f/2 lens, analyzed by a double grating infrared spectrometer and detected by a very sensitive Hg:Ge photoconductor. The evidence for optical mixing was obtained by the observation of a new line in the forward scattered light around 11 μ which is produced by Thomson scattering of the 10.27 μ line from the EPW generated by the beat wave. Moreover, this radiation was only generated when $\omega_p = \Delta\omega$ as shown in Fig. 5. Although the FWHM of the input laser pulse was 75 ns the 11 μ line was only about 25 ns wide. Another unusual and at first rather puzzling effect was observed. Whenever $\Delta\omega = \omega_p$, very strong refraction of the beam occurred outside the cone angle of the incident beam. (Fig. 6) This phenomenon has been called resonant self-focusing due to the ponderomotive force of the EPW.[14]

The ponderomotive force F_{NL}(plasmon) can be much larger than F_{NL}(light). The amplification factor A is given by

$$A = \frac{F_{NL}(\text{plasmon})}{F_{NL}(\text{light})} = \frac{-\nabla\langle E_p^2\rangle/8\pi}{-(\omega_p^2/\omega_o^2)\ \nabla\ \langle E_o^2\rangle/8\pi}, \qquad (7)$$

E_p is the electric field of the EPW. Poisson's equation gives $E_p = 4\pi e n_1/k_p$ and since $v_o = eE_o/m\omega_o$ and $v_p = c$ we obtain the amplification factor

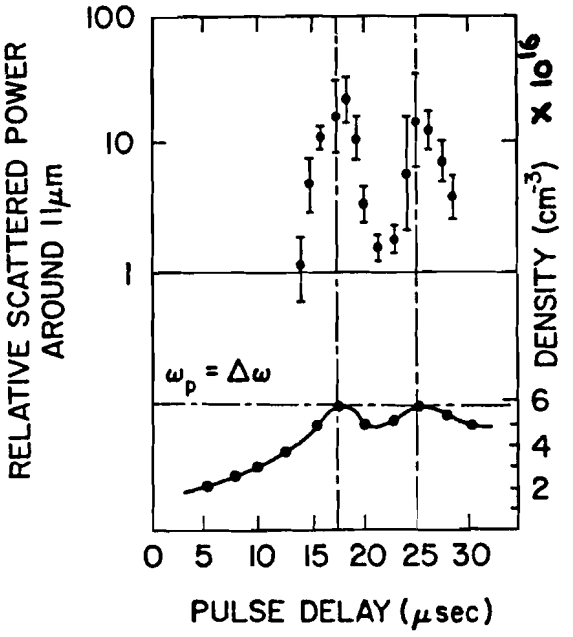

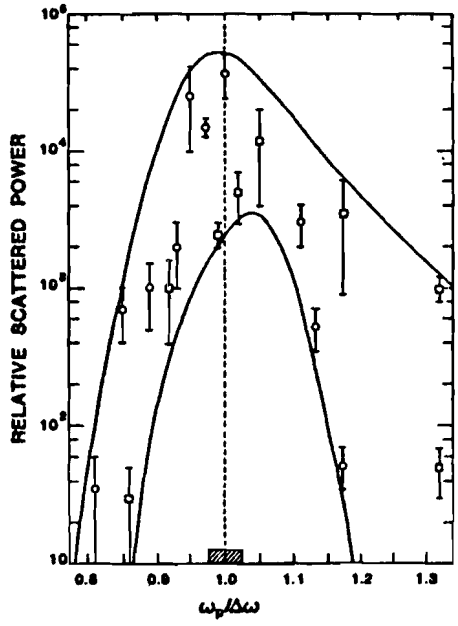

Fig. 5. Time evolution of the arc density and scattered power in frequency $\omega_2 = (10.27\ \mu) - \omega_p$.

Fig. 6. Forward refracted light in the 10.27 μ line vs. $\omega_p/\Delta\omega$ with density measured by ruby interferometry (□) and by Stark broadening of a seed gas H_α line. The shaded areas indicate the spread of difference frequencies in the incident beam.

$$A = \left(\frac{v_p}{v_o}\ \frac{n_1}{n_o}\right)^2 = \left(\frac{n_1/n_o}{v_o/c}\right)^2 . \qquad (8)$$

Using the value of $n_1/n_o \approx 0.4\%$ estimated from the absolute levels of Thomson scattered light from the EPW and $I_o = 10^{10}$ W cm^{-2} we obtain $A > 20$. Since the wavelength of the EPW is about the same as the diameter of the focal spot, the longitudinal and transverse gradients of the electric fields are comparable and a density depression is created on axis which causes deflection of the beam by refraction. It is not clear whether the amplitude of the EPW in this experiment was limited by relativistic effects or ion dynamics, however, the time duration of the EPW was almost certainly limited by the ion motion. The wave potential corresponding to $n_1/n_o \sim 0.4\%$ was about 2.5 kV, i.e. $<< mc^2$ and since T_e was only 5 eV no hot electrons due to trapping were expected. However, this experiment did demonstrate that a short k_p EPW can be generated resonantly via the optical mixing process. More experiments are needed to check out the predictions of the optical mixing theory at low laser powers, perhaps with shorter laser pulses.

The role of RFS instability in hot electron generation was investigated in another experiment.[15] 130 Å thick, self-supported carbon foils were irradiated at normal incidence by intense; $v_o/c \sim 0.3$, 700 ps FWHM, CO_2-laser pulses. 1-5% of the incident energy was backscattered and roughly 50% of the incident energy was transmitted by the plasma. Thus it

can be assumed that the foil plasma becomes underdense around the peak of the laser pulse. The electron temperature of the bulk distribution was deduced from the slope of the ion spectra recorded absolutely using Thomson parabolas, to be ~20 keV for both front and rear expansions. The angular distribution of the electrons escaping the plasma was measured using two absolutely calibrated electron spectrometers in the range 0.4-1.5 MeV.

Fig. 7 shows the absolute electron spectra measured at $\theta \simeq 5^{o}$ in the forward direction and $\theta \simeq 15^{o}$ in the backward direction from the thin carbon foil plasmas. If a Maxwellian distribution is assumed then these distributions can be characterized by temperatures of 90-100 keV in the forward direction and of 40-50 keV in the backward direction. Electrons with energies up to 1.4 MeV were observed in the forward direction. The highest energy electron emission (> 1 MeV) was strongly peaked in the direction of the laser. Electrons up to 400 keV were observed nearly isotropically, however, probably attributable to $2\omega_p$ decay and Raman sidescattering. Integrating over the measured angular distribution, assuming azimuthal symmetry, ~10^{11} electrons with energy greater than 400 keV were found to escape the plasma. Although no direct measurements of the target potential due to this loss of electrons were made, we note that target potentials of ~200 keV have been measured under similar irradiance conditions.[16]

A simple estimate shows that RFS is important in our experiment. The growth rate for the RFS process [17] is given by $\gamma = \frac{1}{2}(v_o/c)\omega_p^2/\omega_o$ and the finite length limit on growth is $\gamma L/(cv_g)^{\frac{1}{2}} > 1$, where $v_g = {}^{p}3\, k_p v_e^2/\omega_p$, and L is the interaction length. Assuming $v_o/c \sim 0.3$, $T_e \sim 20$ keV, $\omega_p/\omega_o \sim 0.46$, we obtain for $L/\lambda \sim 50$, $\gamma/\omega_o \sim 0.03$ and we have nearly 27 e-folding growths from the initial noise level. For backscatter the growth rates are comparable to those for the forwardscatter but backscatter suffers much more

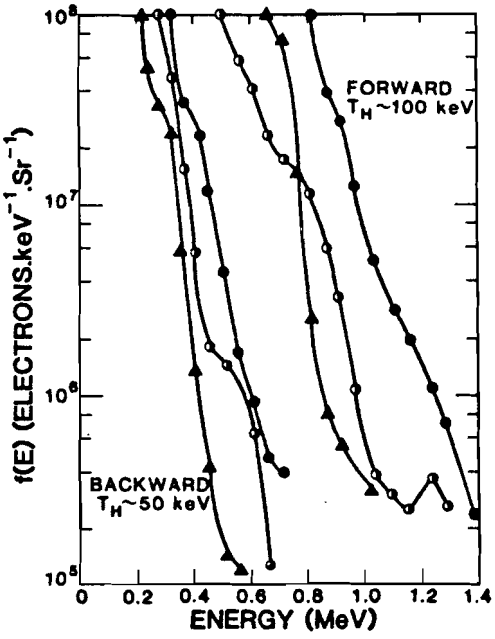

Fig. 7. Experimental electron energy distributions in the forward and backward directions from thin C foil plasmas.

severe Landau damping due to the shorter wavelength and the lower phase velocity of the backward EPW. The assumption of a homogeneous plasma with $L/\lambda \sim 50$ is reasonable, since we expect the instability to occur in the density plateau region, separating the front and the rear expansions. This region has a density scalelength somewhere in between the focal spot diameter (150 μ) and the ion acoustic speed times the FWHM pulse length (1000 μ). In any case the depth of focus of the laser beam was ~50 wavelengths.

Simulations were carried out on the 1D relativistic electromagnetic particle code[11] with the periodic boundary conditions where similar wave setups were used as in reference 1. The plasma was initially thermal, $T_e \sim 20$ keV and uniform, $\omega_p/\omega_o \sim 0.46$. The propagating electromagnetic pulse had a $v_o/c \sim 0.3$. The distribution function $f(P_{||})$ as well as the electrostatic wave spectra are displayed in Fig. 8. The temperature and the maximum electron energy observed in the simulation distributions were similar to the experimentally measured values. For instance, simulations show electrons with $(\varepsilon_{max})_F \simeq 1.3$ MeV and $(T_{HOT})_F \sim 100$ keV in the forward direction compared to experimental values $(\varepsilon_{max})_F \sim 1.4$ MeV and $(T_{HOT})_F \sim 90$-100 keV. Similarly, simulations show $(\varepsilon_{max})_B \sim 0.9$ MeV and $(T_{HOT})_B \sim 60$ keV in the backward direction compared to experimental values of $(\varepsilon_{max})_B \sim 0.8$ MeV and $(T_{HOT})_B \sim 40$-50 keV. In view of the possible influence of the target potential on the experimentally measured electron distributions, this rather excellent agreement between the experiment and the simulations may be rather fortuitous, particularly for the maximum electron energy unless the target potential was indeed much smaller than ε_{max}. The electrostatic wave spectra (Fig. 8b) shows that the backscatter mode k_b (which grows initially) is swamped by other modes with a smaller wave number, the most intense of which is the plasma wave associated with forwardscatter k_p. In addition, there are some wavenumbers which are less than k_p. Thus the heated electron distributions obtained by the experiment and the simulations agree well with most of the electron heating due to the RFS process (and/or multiple RFS processes since repeated k matching is possible only for the RFS process), but is not so much due to the backward process.

The reason why the backscattering is suppressed is the following: When the backscattering EPW is excited, heavy Landau damping or electron trapping

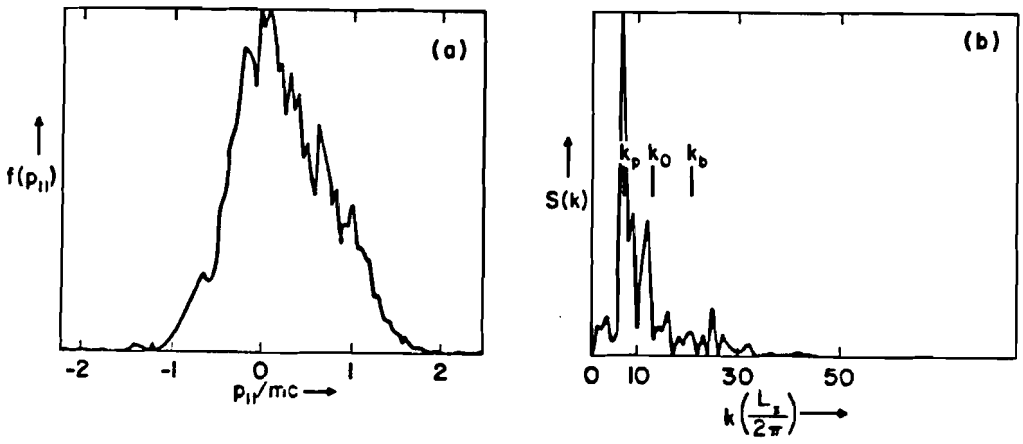

Fig. 8. Simulation (under the same conditions as in Fig. 7) of electron energies (a) at $t = 250\ \omega_p^{-1}$ as well as (b) the electrostatic mode spectra at $t = 100\ \omega_p^{-1}$.

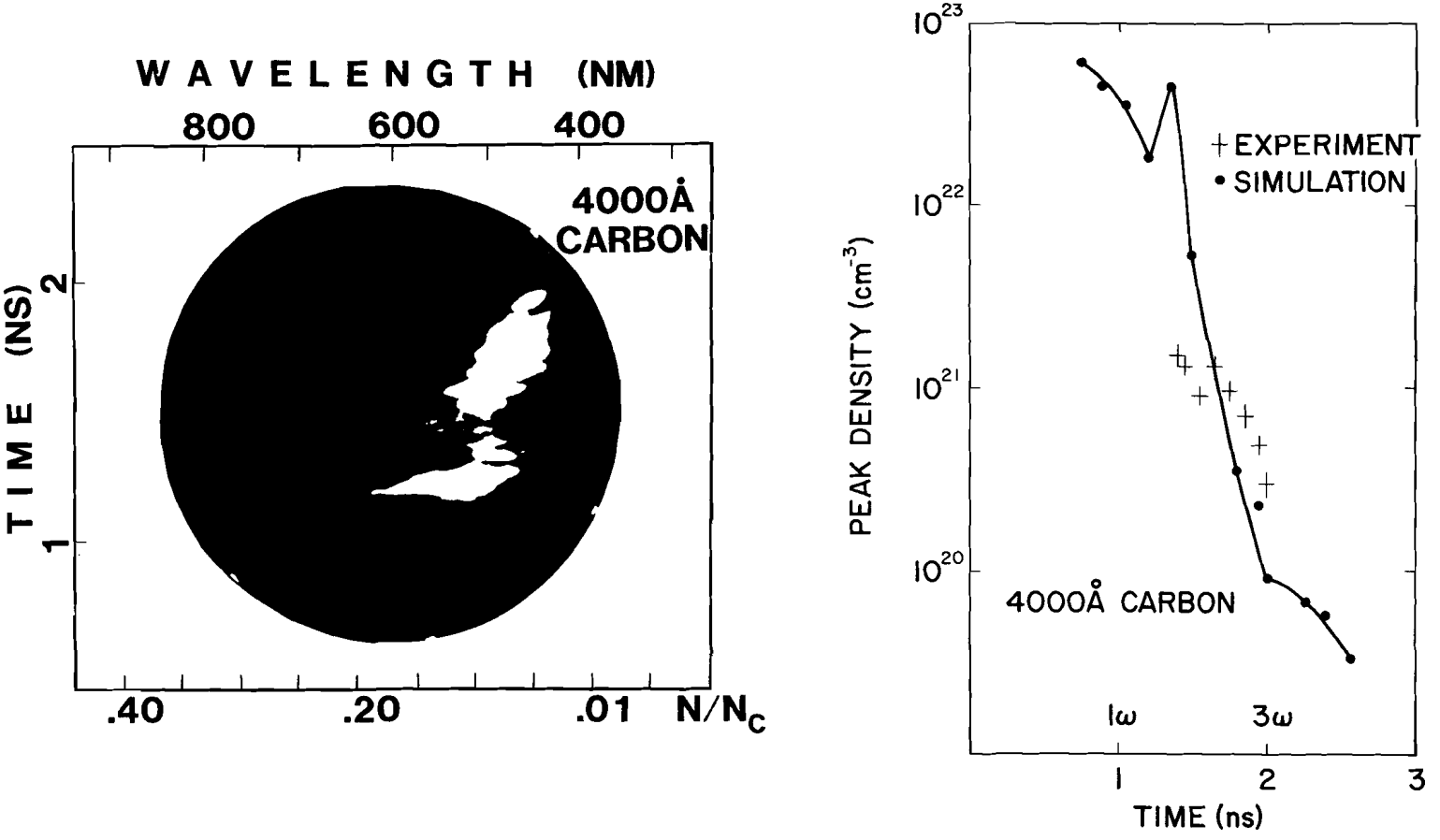

Fig. 9. (a) A typical streak record of Raman backscattered light from a 4000 Å thick carbon foil plasma and,
(b) comparison between experimentally obtained maximum plasma density and 2D LASNEX prediction. Times 1 ns and 2 ns correspond to peaks of the 1 μm prepulse and 0.35 μm mainpulse respectively.

by this EPW saturates it at a low level thus limiting the backscattering to a small value. The phase velocity of the backscattering EPW $v_p = \omega_p/k_p$ which for this case is ~1.6 v_e. Thus this wave is heavily Landau damped to begin with and as it grows in amplitude, more and more particles will be trapped by it and the damping will grow. The trapping width is given approximately by $\Delta v_t = (2eE_{EPW}v_p/m\omega_p)^{\frac{1}{2}}$, where E_{EPW} is the electric field for the plasma wave. The condition that a large number of electrons are trapped is given[9] by $v_p - \Delta v_t \lesssim 2v_e \equiv 2(T_e/m)^{\frac{1}{2}}$. The maximum electrostatic wave intensity is obtained for a cold plasma by setting $v_e = 0$. This gives for the saturation amplitude E_{EPW} for the longitudinal wave as $(eE_{EPW}/m\omega_p) = v_p/2$. For our case, the phase velocity is $0(v_e)$ and we expect little growth; in any case, the saturation intensity for a cold plasma is less than 6% of the light waves. In addition the two plasmon decay instability would also saturate at a low level even if ω_o were chosen to be $2\omega_p$ because strong Landau damping sets in much earlier for $2\omega_p$ decay than it does for the forward Raman process. The RFS process appears to be the last parametric process to saturate in this hot underdense plasma.

Recently, we have been exploring the possibility of producing ultra-high electric fields on the order of half-TeV per meter by using a short wavelength ultra-violet laser to drive the RFS instability in a high density underdense plasma. The maximum energy gain by a trapped particle is simply a function of the plasma density to the critical density ratio ($E_{max} \sim 2\gamma^2mc^2 \sim 2(\omega_o/\omega_p)^2 mc^2 \sim 2n_c/n\ mc^2$). This is because although the electric field is higher at a shorter wavelength, the wavelength of the electron plasma wave is shorter and the $\int \underline{E}\cdot d\underline{\ell}$ is a constant. Thus by going to a shorter wavelength the main gain is in obtaining the same energy in a much shorter distance compared to when a long wavelength laser is used. For example, if we use a 0.35 μ laser, (third harmonic of 1 μ glass laser) then for a density ratio n_c/n of 10^3 we may expect to achieve 1 GeV electrons over an incredibly short distance of only 3.5 mm instead of ~10 cm for a 10.6 μ CO_2 laser. At shorter wavelengths we might also expect a much higher beam luminosity since the plasma density is higher.

In exploratory experiments, carried out at the National Laser Users' Facility of the University of Rochester, 4000 Å thick carbon foil targets were irradiated by a low intensity (10^{12} W/cm^2) 1 μ prepulse to produce a preformed underdense plasma. The 0.35 μ mainpulse, 10^{15} W/cm^2, was tightly focused at the center of the preformed plasma by an f/12 lens to excite the RFS instability. The mainpulse and the prepulse were delayed by 1 nsec to allow the preformed plasma to expand and establish a reasonable density scalelength. The plasma temperature was ~700 eV and length was ~150 laser wavelengths. Raman backscattering instability was excited during the rise-time of the 3ω laser pulse as evidence by the time resolved Raman back-scatter spectrum shown in Fig. 9(a). The shift of the long wavelength cut-off of the Raman backscatter spectrum to the blue is due to the plasma density decreasing as a function of time because of the frequency matching condition. Fig. 9(b) shows the comparison of the experimentally measured peak density and the results of a 2D hydrodynamic simulation of our experiment using the code LASNEX. The critical density for 0.35 μ laser light is 9×10^{21} cm^{-3}. It can be seen that a plasma with $n_c/n \sim 10^2$ was produced at the peak of the 0.35 μ laser pulse. Unfortunately, the laser intensity was not sufficient, or the plasma density scalelength long enough to excite the fast wave ($v_p \sim c$) characteristic of the RFS instability. We observed high energy electrons with energies out to 350 keV but their angular distribution and polarization dependence suggested $2\omega_p$ decay as the generation mechanism. We are continuing experiments along these lines to exploit the potential of short-wavelength lasers for producing ultra-high electric fields.

FUTURE EXPERIMENTS

The two experiments described in this paper have demonstrated the following:

(a) Using a multiline CO_2 laser of only 10^{10} Wcm^{-2}, electron density fluctuations can be reasonantly excited for up to 25 ns.

(b) When an intense CO_2 laser pulse is incident on a hot, tenuous plasma, relativistic energy electrons can be produced in the direction of the laser beam. The energy distribution of these hot electrons is not monoenergetic but is rather Maxwellian.

In addition, we have been looking at the use of short wavelength lasers for producing ultra-high electric fields propagating close to the speed of light. This is just the beginning. Crucial experiments need to be done which combine the phenomena of optical mixing and RFS to check how the maximum electron energy scales with v_o/c, ω_p/ω_o and the depth of the focus of the laser beam. Computer simulations described in the paper by Tajima[19] would suggest rather a weak dependence on the laser intensity provided the RFS threshold is exceeded. On the other hand the maximum energy in simulation scales as $(\omega_o/\omega_p)^2$, i.e., inversely proportional to the plasma density. Similarly the Thomson scattering diagnostic described in this paper needs to be exploited to obtain the complete electrostatic wave spectrum $S(k, \omega)$ generated in the two beam case and compare it to the simulation spectrum. It is also of some importance to investigate to what extent two dimensional effects such as sidescattering and bubble formation are important. Another crucial question that may be more conveniently addressed to in simulations is 'how important is the background temperature of the plasma in determining the relative importance of Landau damping and particle trapping?' Experiments designed to answer these questions should form the next stage of research on the plasma beat wave accelerator. If the results look promising and very large longitudinal electric fields can indeed by produced using existing 1 μ or 10 μ laser facilities, then it would be of enormous interest to see if an externally injected, nearly monoenergetic beam of electrons or protons can be accelerated to GeV(s) while keeping it relatively monoenergetic.

ACKNOWLEDGEMENTS

I wish to acknowledge the contribution my colleagues; C. Clayton, Dr. F. F. Chen, Dr. N. A. Ebrahim, Dr. H. A. Baldis, H. Figueroa and Dr. K. Estabrook, gave in successfully carrying out the work described in this paper. Stimulating discussions with T. Tajima and D. Sullivan are acknowledged with pleasure.

This work was supported by DOE contracts: DE-AS08-81DP40163, DE-AS08-81DP40135, DE-AS08-81DP40166 and NSF grant ECS-80-03558.

REFERENCES

1. T. Tajima and J. M. Dawson, Phys. Rev. Lett. 43, 267 (1974).
2. B. I. Cohen, A. N. Kaufman, and K. M. Watson, Phys. Rev. Lett. 29, 581 (1972).
3. N. A. Ebrahim, C. Joshi and H. A. Baldis, Phys. Rev. A 25, No. 4 (1982).
4. N. Krall, A. Ron and N. Rostoker, Phys. Rev. Lett. 13, 83 (1964), G. Weyl, Phys. Fluids 13, 1802 (1970).
5. M. N. Rosenbluth and C. S. Liu, Phys. Rev. Lett. 29, 701 (1972).
6. K. Estabrook, W. L. Kruer and B. F. Lasinski, Phys. Rev. Lett. 45, 1399 (1980).

7. W. L. Kruer, K. Estabrook, B. F. Lasinski and A. B. Langdon, Phys. Fluids 23, 7 (1980).
8. K. Estabrook in Laser Program Annual Report UCRL-50021-80, Vol. 2, p. 3-34 (1980), Lawrence Livermore National laboratory.
9. J. M. Dawson and R. Shanny, Phys. Fluids 11, 1506 (1968).
10. This formula is nonrelativistic but is illustrative for the present purpose.
11. A. T. Lin, J. M. Dawson and H. Okuda, Phys. Fluids 17, 1995 (1974).
12. M. Ashour-Abdalla, J. N. Laboeuf, T. Tajima, J. M. Dawson and C. F. Kennel, Phys. Rev. A23, 1406 (1981).
13. B. L. Stansfield, R. Nodwell and J. Meyer, Phys. Rev. Lett. 26, 1219 (1971).
14. C. Joshi, C. E. Clayton and F. F. Chen, Phys. Rev. Lett. 48, 874 (1982).
15. C. Joshi, T. Tajima, J. M. Dawson, H. A. Baldis and N. A. Ebrahim, Phys. Rev. Lett. 47, 1285 (1981).
16. R. F. Benjamin, G. H. McCall and A. W. Ehler, Phys. Rev. Lett. 42, 890 (1979).
17. J. J. Thomson, Phys. Fluids 21, 2082 (1978).
18. H. Figueroa, C. Joshi, C. Clayton, H. Azechi, N. A. Ebrahim and K. Estabrook, University of California, Los Angeles, PPG-674. To be published in Laser Interaction and Related Plasma Phenomena, Vol. 6. Ed. G. Miley and H. Hora, Plenum Press.
19. T. Tajima-Proceedings of this conference.